Journal of Electrochemical Science and Technology
Vol. 3, No. 4, 2012, 172-177
http://dx.doi.org/10.5229/JECST.2012.3.4.172

Journal of Electrochemical Science and Technology

Effect of Mo-doped $LiFePO_4$ Positive Electrode Material for Lithium Batteries

Seung-Min Oh[b] and Yang-Kook Sun[a,b,†]

[a]*Department of Energy Engineering, Hanyang University, Seoul 133-791, South Korea*
[b]*Department of Chemical Engineering, Hanyang University, Seoul 133-791, South Korea*

ABSTRACT :

Mo-doped $LiFePO_4$ was synthesized via co-precipitation method using sucrose as the carbon source. Structure, surface morphology, and the electrochemical properties of the synthesized olivine compounds were investigated using Rietveld refinement of X-ray diffraction data (XRD), scanning electron microscopy (SEM), and electrochemical charge-ischarge tests. Spherical morphology with the particle size of ~8 μm authenticated the enhanced tap density and volumetric energy density of the synthesized materials. Charge-discharge behavior of $LiFePO_4$ and Mo-doped $LiFePO_4$ cells demonstrated a specific capacity of 130 and 145 mAh g^{-1}, respectively. Mo-doped $LiFePO_4$ cells exhibited an excellent discharge capacity at 96 mAh g^{-1} at 7 C-rate.

Keywords: Co-precipitation, Doping, Electrochemical properties, Lithium- ion Battery, Olivine

Received December 9, 2012 : Accepted December 23, 2012

1. Introduction

Lithium batteries are the system of choice, offering high energy density, flexible and lightweight design, and longer lifespan than comparable battery technologies.[1)] The role and the demand for lithium ion batteries are expanding in the mid-large scale battery system; such as, electric vehicles (hybrid electric vehicles), energy storage devices, and electronic devices. . The major share as a positive electrode material in the lithium battery market is being occupied by the transition metal oxides[2-4)] that experiences several shortcomings associated with material usage, cost and performance inevitability.

For these reasons, many research groups studies on olivine type materials in particular to $LiFePO_4$ is being carried out as positive electrode materials for lithium batteries.[5-7)] $LiFePO_4$ as a positive electrode material in rechargeable lithium batteries offers an excellent theoretical capacity (170 mAh g^{-1}) with enhanced deliverable capacity (> 95% of the theoretical capacity), structural stability, and environmental friendly.[8)] However, poor electronic conductivity (< 10^{-9} S cm^{-1}) of $LiFePO_4$ has been an issue for commercialization of olivine material as positive electrode material for Li-ion battery application.[9)] Many efforts are made over the years to overcome the intrinsically low electronic conductivity of the material, which includes optimization of synthesis procedures,[10)] surface modification via carbon coating[11)] and other metal oxides,[12)] electronic modification by doping.[13,14)]

Nano- sized $LiFePO_4$ could effectively shorten the diffusion pathway of lithium ions, resulting in enhanced rate capability and utilization. Furthermore, a well-dispersed electrically conductive carbon phase on nano-sized particles could improve the electronic conductivity. However, nano-sized particles have an inevitable disadvantage of low tap-density due to the unique property of their large surface areas, which results in low volumetric capacity. In this work, the synthesis of high tap-density C-$LiFePO_4$ with an 8-

†Corresponding author. Tel.: +82-2-2220-0524
E-mail address: yksun@hanyang.ac.kr

micron particle size is reported, and the effect of $LiFePO_4$ particle size (tap-density) on the electrochemical performance of the gravimetric capacity was investigated. Additionally, the effects of Mo doped on the crystal structure and electrochemical properties of the micron-sized C-$LiFePO_4$ with a high tap-density of 1.5 g cm^{-3} are presented.

2. Experimental

$LiFePO_4$ and Mo-doped $LiFePO_4$ materials were synthesized via co-precipitation method. Starting materials, $Fe(NO_3)_3 \cdot 9H_2O$ and H_3PO_4, were first dissolved in distilled water with a molar ratio of 1:1 with respect to Fe:P, respectively. Then, the aqueous solution with a concentration of 2.0 M, was pumped into a continuously stirred tank reactor (capacity: 4 L, feeding rate: 300 ml h^{-1}). An aqueous NH_4OH solution was pumped into the reactor to control the pH of the solution, simultaneously. The concentration of metal (calculated by feeding rate and concentration of metal solution, concentration reached to 2.0 M after stabilization), pH (2), temperature (50°C) and stirring speed (1000 rpm) of the mixture in the reactor were monitored and controlled during the reaction process, because these conditions affect the nucleation and particle growth from the precursor. As a result, yellow colored precipitates were immediately formed after the NH_4OH solution was pumped into the reactor. The reaction temperature was kept to 50°C throughout the reaction. As-received $FePO_4$ hydrates were filtered, washed and vacuum-dried at room temperature. It was then heat treated at 550°C for 10 h in an Ar atmosphere to obtain anhydrous $FePO_4$ powders (hereafter referred to as precursor). The obtained precursor was thoroughly mixed with a stoichiometric amount of Li_2CO_3, MoO_3 and sucrose (the molar ratio Li:Mo:Fe:P was 0.99:0.01:1:1) to produce carbon-coated $LiFePO_4$ and Mo-doped $LiFePO_4$. Those mixtures were then calcined at 800°C for 15 h (heating rate: 5°C min^{-1}) under a restricted atmosphere (Ar/H_2:96/4 by volume %).

The crystalline phase of the synthesized olivine material was characterized by Powder X-ray diffraction (XRD, Rint-2000, Rigaku) measurement using Cu-Kα radiation. Particle morphologies of the precursor and the powders were observed using scanning electron microscopy (SEM, JSM 6400, JEOL). An elemental analyzer (EA, EA110, CE Instrument) was employed to determine the amount of carbon in the final products.

Positive electrodes were fabricated using a mixture of prepared powders (85 wt.%), carbon black (7.5 wt.%), and polyvinylidene fluoride in *N*-methylpyrrolidinon (NMP) (7.5 wt.%). The loading of the active material per unit area of 6.5 mg cm^{-2} and the electrode thickness of 43.3 μm . The slurry was spread onto Al foil and dried in an oven at 80°C. The electrode was dried over-night at 120°C under vacuum and then roll-pressed prior to use. Electrochemical properties of the prepared $LiFePO_4$ were measured using CR2032 coin-type cells with a Li metal anode. The electrolyte solution was 1M $LiPF_6$ in a 1:1 volume mixture of ethylene carbonate (EC) and diethyl carbonate (DEC) (PANAX ETEC., Korea). Construction of the coin cells was carried out in an argon-filled glove box. The cells were cycled galvanostatically at a 0.1 C rate (0.1 C = 17 mA g^{-1}) in a voltage range of 2.5-4.3 V vs. Li at 25°C. AC-impedance measurements were performed using a Zahner Elektrik IM6 impedance analyzer over the frequency range from 1 MHz to 1 mHz with an amplitude of 10 mV_{rms}.

3. Results and Discussions

Fig. 1 shows Rietveld refinement results of XRD data for $LiFePO_4$ and Mo-doped $LiFePO_4$. Sharp and well-defined Bragg peaks ensures the highly crystalline for both products. That is, both $LiFePO_4$ and Mo-doped $LiFePO_4$ exhibit a well-ordered orthorhombic olivine type structure with *Pnma* space group. To follow where the Mo element exists in the $LiFePO_4$ structure, Rietveld refinements for both compounds were carried out. For the Mo-doped one, we assumed three possibilities: i) full occupation of Li octahedral (4a) site, ii) full occupation of Fe octahedral site (4c) site, and iii) occupation of both Li and Fe octahedral sites. For $LiFePO_4$, the observed and calculated patterns fit well, which means that all elements are well located in their sites as shown in Table 1. For Mo-doped $LiFePO_4$, we could also obtain well-refined patterns in Fig. 1(b). We postulated three possibilities, but the case 3 resulted in the highest reliable factors as described in Table 2. The refined chemical composition can be written as $[Li_{0.946}Mo_{0.016}\square_{0.038}][Fe_{0.988}Mo_{0.004}\square_{0.008}]PO_4$. ($\square$ = vacancy) Zhang *et al.*[15] suggested that Mo^{6+} tends to occupy the Li (4a) sites due to its smaller ionic radius in octahedral coordination than Fe^{2+}. Generally, it is believed that difference in ionic

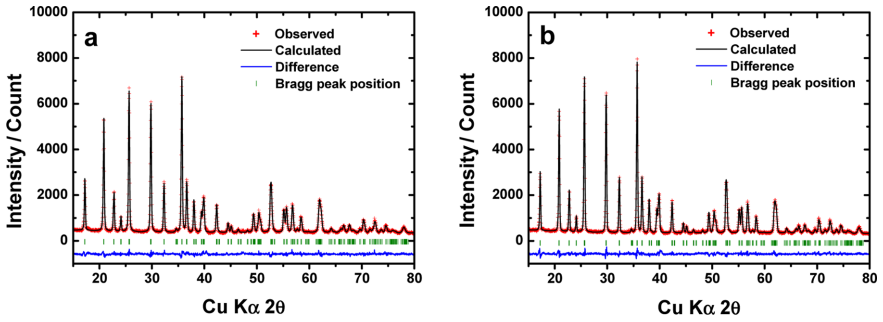

Fig. 1. XRD patterns of as-synthesized (a) $LiFePO_4$ and (b) Mo-doped $LiFePO_4$.

Table 1. Cell parameters of $LiFePO_4$ obtained from Rietveld refinement of XRD data

Formula		$LiFePO_4$				
Crystal system		Orthorhombic				
Space group		Pnma				
Atom	Site	x	y	z	g	B/Å^2
Li1	4a	0	0	0	1	2.44
Fe	4c	0.283(1)	0.25	0.973(4)	1	1.60
P	4c	0.095(2)	0.25	0.419(6)	1	1.46
O1	4c	0.095(6)	0.25	0.742(14)	1	1.74
O2	4c	0.456(6)	0.25	0.207(9)	1	0.63
O3	8d	0.164(4)	0.050(7)	0.282(6)	1	0.93
R_{wp}/%		9.65				
R_p/%		9.12				
R_{Bragg}/%		3.13				
Cell parameters		a = 10.3116(2) Å b = 5.9978(1) Å c = 4.6883(1) Å				

Table 2. Cell parameters of Mo-doped $LiFePO_4$ obtained from Rietveld refinement of XRD data

Formula		$Li_{0.946}Mo_{0.016}Fe_{0.988}Mo_{0.004}PO_4$				
Crystal system		Orthorhombic				
Space group		Pnma				
Atom	Site	x	y	z	g	B/Å^2
Li	4a	0	0	0	0.946(2)	2.31
Mo1	4a	0	0	0	0.016(2)	2.31
Mo2	4c	0.282(1)	0.25	0.973(4)	0.004(1)	1.64
Fe	4c	0.282(1)	0.25	0.973(4)	0.988(1)	1.64
P	4c	0.095(3)	0.25	0.418(6)	1	1.53
O1	4c	0.095(7)	0.25	0.739(14)	1	1.74
O2	4c	0.455(7)	0.25	0.203(10)	1	0.63
O3	8d	0.167(5)	0.048(7)	0.287(7)	1	0.93
R_{wp}/%		10.0				
R_p/%		9.72				
R_{Bragg}/%		3.24				
Cell parameters		a = 10.3066(3) Å b = 5.9957(1) Å c = 4.6879(1) Å				

radius should be within 15% to make a successful substitution or doping. In consideration of the ionic radius of Mo^{VI} (0.59 Å) against Li^{I} (0.76 Å) or Fe^{II} (0.78 Å), the Mo^{VI} is too small to replace the Li^{I} ingredient. For this reason, ionic radius for the dopant should be greater than that of hexavalent Mo element. When the larger Mo ions (Mo^{III} (0.69 Å) and/or Mo^{IV} (0.65 Å) are incorporated into the olivine $LiFePO_4$ structure, it satisfies size effect and the valence state of the structure even though vacancies are generated.[16] Barker *et al.*[17] synthesized $LiMoO_2$ at highly reductive atmosphere (carbothermal method), of which the valence of Mo is 3+. This indicates that formation of lower valence Mo is also possible. Due to the incorporation of the smaller ions into the structure, the resulting lattice parameters were slightly decreased comparing with those of $LiFePO_4$. Similar results were also reported by Zhang *et al.*[15] The amount of carbon remaining in the final $LiFePO_4$ and Mo doped-$LiFePO_4$ was 2.93 wt.% and 2.92 wt.%, respectively, as confirmed by a CHN analyzer. Surface morphology of the synthesized materials was examined by a field-emission scanning electron microscopy. Fig. 2(a)-(b) shows the as-synthesized $LiFePO_4$ and Mo-doped $LiFePO_4$. The spherical particle size of ~8 μm was observed, where the primary particles was estimated as submicron size. Hu *et al.*[18] suggested that heat-treatment above 700°C resulted in particles to fuse together partially to form large porous agglomerates regardless of the optimizations adopted. In our experiment, neither fusion of particle nor particle

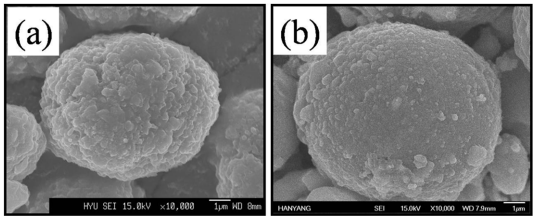

Fig. 2. SEM images of (a) $LiFePO_4$ and (b) Mo-doped $LiFePO_4$.

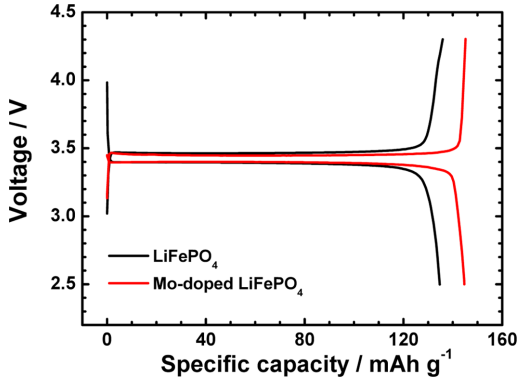

Fig. 3. Initial charge-discharge voltage profiles of $LiFePO_4$ and Mo-doped $LiFePO_4$ cells cycled between 2.5 and 4.3 V at a constant current density of 17 mA g^{-1}.

agglomeration was found for both materials. As conferred from our earlier investigations,[19] existence of uneven particles with particle agglomeration obviously reduces the packing degree and tap density. Ying *et al.*[20] recently reported that the presence of spherical particles gave a significant improvement in the resulting specific volumetric capacity of $LiFePO_4$. The tap-densities of the both samples are *ca.* 1.5 g cm^{-3} which are larger than nano-sized $LiFePO_4$ powders (0.6 g cm^{-3}). We convince from the particle morphology that both $LiFePO_4$ and Mo-doped $LiFePO_4$ would have higher volumetric capacity.

Fig. 3 shows the 1st cycle charge/discharge curves of $LiFePO_4$ and Mo-doped $LiFePO_4$ composite positive electrodes examined at room temperature under a constant current density of 17 mA g^{-1} in a potential window of 2.5-4.3 V. Both $LiFePO_4$ and Mo-doped $LiFePO_4$ composites displayed a long voltage plateau at 3.5 V, which is the typical characteristic behavior of lithium iron phosphate.[19] This potential plateau is also ascribed to the two phase reaction occurring between $FePO_4$ and $LiFePO_4$ due to the process of reversible Li^+ ion insertion/extraction into and out of the olivine structural matrix as suggested by several researchers.[8,11,13] In Fig. 3, the Mo-doped $LiFePO_4$ exhibited an initial discharge capacity of 145 mAh g^{-1} against 130 mAh g^{-1} demonstrated by the $LiFePO_4$. Furthermore, the partial substitution of Mo for Li would be effective in enhancing the electrical conductivity of the olivine particles, as suggested by Zhang *et al.*[15]

Differential capacity versus voltage plots of the 1st and 5th cycle of the $LiFePO_4$ and Mo-doped $LiFePO_4$ are presented in Fig. 4(a) and (b). The synthesized compounds had a set of oxidation and reduction peaks in the potential range of 2.5-4.3 V versus Li. For Mo-doped one, we could observe slightly lower charge voltage and the resulting discharge voltage also appeared at a little higher voltage in Fig. 4(a) and (b). This implies that resistance was reduced by incorporation of Mo into the $LiFePO_4$ structure. The differences of oxidation and reduction peaks voltage for the Mo-doped $LiFePO_4$ were smaller than those for the $LiFePO_4$, which may be ascribed to the improved kinetics of the Mo-doped $LiFePO_4$ composite. We also performed the cyclic voltammetry of the both $LiFePO_4$ samples with scan rate of 0.5 mV s^{-1} in Fig. 4(c). From this result, the chemical diffusion coefficient of the Li ion in $LiFePO_4$ and Mo-doped $LiFePO_4$ obtained using the Randles-Sevcik equation (Eq. 1) from previous paper.[25]

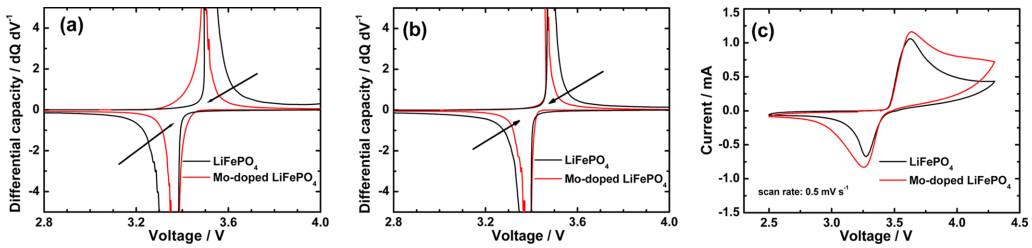

Fig. 4. Differential capacity vs. voltage plot of $LiFePO_4$ and Mo-doped LiFePO4: (a) 1st cycle and (b) 5th cycle. (c) Cyclic voltammetry profiles of $LiFePO_4$ and Mo-doped $LiFePO_4$

Table 3. Chemical diffusion coefficient of $LiFePO_4$ and Mo-doped $LiFePO_4$ obtained from CV

	$LiFePO_4$	Mo-doped $LiFePO_4$
Anodic D ($cm^2\ s^{-1}$)	4.19×10^{-16}	5.05×10^{-16}
Cathodic D ($cm^2\ s^{-1}$)	1.69×10^{-16}	2.59×10^{-16}

$$I_p/m = 0.4463F(F/RT)^{1/2}C_{Li}V^{1/2}AD^{1/2} \quad (1)$$

where I_p is the peak current in amperes (A), m is mass of electrode (g), F is the Faraday constant, C_{Li} is the initial concentration of Li (mol cm^{-3}), V is scan rate (V s^{-1}), A is electrode area (cm^2), D is the diffusion constant ($cm^2\ s^{-1}$). We confirmed that the Li ion diffusion coefficient of Mo-doped $LiFePO_4$ is larger than $LiFePO_4$ sample which is well matched with differential capacity result (Table 3).

Cyclability of the $LiFePO_4$ and Mo-doped $LiFePO_4$ is shown in Fig. 5. A constant current density of 17 mA g^{-1} (0.1 C) was applied. The $LiFePO_4$ and Mo-doped $LiFePO_4$ composites delivered an initial discharge capacity of 130 and 145 mAh g^{-1} at room temperature, respectively. It was observed that discharge capacities of both tested cells were slightly increased and that they were stabilized in the first few cycles. This phenomenon is usually observed in $LiFePO_4$-carbon composites and has been previously reported.[21,22] Mo-doped $LiFePO_4$/Li cell show good capacity retention with high capacity during cycling (100% after 50th cycles).

The effect of Mo substitution on the 0.1-7 C-rate capability between 2.5 and 4.3 V is verified on Fig. 6. The Li/$LiFePO_4$ and Li/Mo-doped $LiFePO_4$ cells were

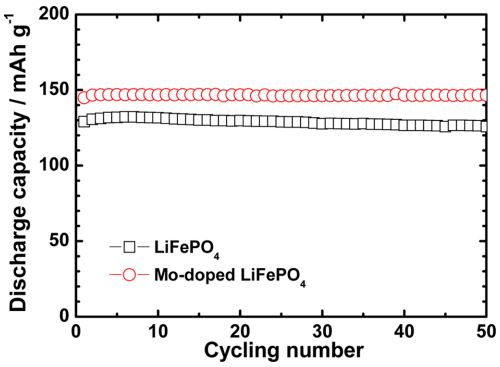

Fig. 5. Capacity versus cyclability plots of $LiFePO_4$ and Mo-doped $LiFePO_4$.

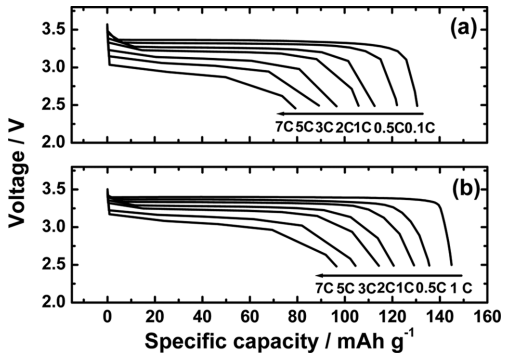

Fig. 6. Rate capability of (a) $LiFePO_4$ and (b) Mo-doped $LiFePO_4$.

charged with a constant current density of 0.1 C-rate (17 mA g^{-1}) before each discharge current rate. With increasing currents, $LiFePO_4$ exhibited a gradual decrease in capacity in Fig. 6(a). However, Mo-doped $LiFePO_4$ exhibited an excellent discharge capacity of 130 mAh g^{-1} at 1 C-rate (170 mA g^{-1}) and 96 mAh g^{-1} at 7 C-rates (1190 mA g^{-1}), which is higher than the $LiFePO_4$ shown in Fig. 6(b). The effect of Mo doping was found to enhance the electrochemical performance of the $LiFePO_4$ both in terms of increased specific capacity and maintenance of capacity upon progressive cycling.

To investigate the possible reason of improved cell performance of the Mo-doped $LiFePO_4$ electrochemical impedance spectroscopy (EIS) for the $LiFePO_4$ and the Mo-doped $LiFePO_4$ were measured after the 10th cycle at 17 mA g^{-1} (0.1 C-rate) at 30°C in Fig. 7. It is

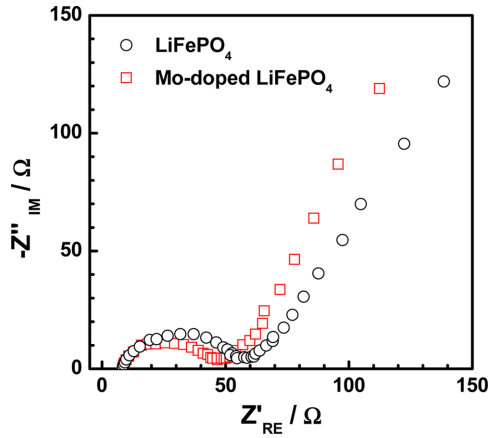

Fig. 7. Cole-Cole plots of $LiFePO_4$ and Mo-doped $LiFePO_4$ after 10th cycle.

composed of a depressed semicircle and a slopping line. The high-frequency semicircle is related to the surface and charge transfer resistance, and the slopping line at the low frequency end corresponds to the Warburg impedance of long range Li-ion diffusion.[23] The equivalent circuit used in this study was reported in our previous study.[24] The surface resistances for both electrodes seem to be close each other in the high to medium frequency range (R_{sf} values of pristine and Mo-doped $LiFePO_4$ are 6.2 Ω and 5.4 Ω, respectively). The Mo-doped $LiFePO_4$ gave rise to the smaller charge transfer resistance relative to $LiFePO_4$ electrode (R_{ct} values of pristine and Mo-doped $LiFePO_4$ are 40.8 Ω and 29.4 Ω, respectively). Therefore, it is concluded that the introduction of Mo-doped $LiFePO_4$ is substantially effective to improve rate and cycling performances of $LiFePO_4$.

4. Conclusions

Micro-scale $LiFePO_4$ and Mo-doped $LiFePO_4$ with spherical morphology were synthesized by the coprecipitation method. Carbon coating was performed using sucrose as the carbon source and percentage of carbon coated to the surface of the olivine particles was maintained at 2.93 wt% ($LiFePO_4$) and 2.92 wt% (Mo-doped $LiFePO_4$), respectively. The formation of phase pure product was evidenced by XRD. An enhancement in the tap density of the materials was substantiated from the formation of exact spherical shaped particles with the particle size distribution of ~8 μm. As expected, the effect of doping was found to enhance the electrochemical performance of the $LiFePO_4$ such as specific capacity and its retention. Hence, the reasonably improved electrochemical performance of Mo-doped $LiFePO_4$ makes it feasible for consideration in high-power lithium-ion battery applications.

Acknowledgements

This work was supported by the National Research Foundation of Korea (NRF) grant funded by the Korea government (MEST) (No. 2009-0092780) and by the Human Resources Development program (No. 20104010100560) of the Korea Institute of Energy Technology Evaluation and Planning (KETEP) grant funded by the Korea government Ministry of Knowledge Economy.

References

1. J. M. Tarascon and M. Armand, *Nature*, **414**, 359 (2001).
2. S. G. Youn, I. H. Lee, C. S. Yoon, C. K. Kim, Y. K. Sun, Y. S. Lee and M. Yoshio, *J. Power sources*, **108**, 97 (2002).
3. J. Reim, H. Rentsch, W. Scheifele and P. Novák, *J. Power Sources*, **174**, 584 (2007).
4. H. Lee, H. J. Kim, D. Kim and S. Choi, *J. Power Sources*, **176**, 359 (2008).
5. A. K. Padhi, K. S. Nanjundaswamy and J. B. Goodenough, *J. Electrochem. Soc.*, **144**, 1188 (1997).
6. D. A. Spong, G. Vitins and J. R. Owenz, *J. Electrochem. Soc.*, **152**, A2376 (2005).
7. T. Nakamura, Y. Miwa, M. Tabuchi and Y. Yamada, *J. Electrochem. Soc.*, **153**, A1108 (2006).
8. A. Yamada, S. C. Chung and K. Hinokuma, *J. Electrochem. Soc.*, **148**, A224 (2001).
9. C. W. Ong, Y. K. Lin and J. S. Chen, *J. Electrochem. Soc.*, **154**, A527 (2007).
10. G. Arnold, J. Garche, R. Hemmer, S. Strobele, C. Vogler and M. W. Mehrens, *J. Power Sources*, **119-121**, 247 (2003).
11. H. Huang, S.-C. Yin and L. F. Nazar, *Electrochem. Solid-State Lett.*, **4**, A170 (2001).
12. H. Liu, G. X. Wang, D. Wexler, J. Z. Wang and H. K. Liu, *Electrochem. Commun.*, **10**, 165 (2008).
13. S. Y. Chung, J. T. Bloking and Y. M. Chiang, *Nat. Mater.*, **2**, 123 (2002).
14. C. H. Mi, X. G. Zhang and H. L. Li, *J. Electroanalytical Chemistry*, **602**, 245 (2007).
15. M. Zhang, L.-F. Jiao, H.-T. Yuan, Y.-M. Wang, J. Guo, M. Zhao, W. Wang and X.-D. Zhou, *Solid State Ionics*, **177**, 3309 (2006).
16. R.D. Shannon, *Acta Cryst.*, **A32**, 751 (1976).
17. J. Barker, M.Y. Saidi, J. L. Swoyer, *Electrochem. Solid-State Lett.*, **6**, A252 (2003).
18. Y. Hu, M. M. Doeff, R. Kostecki and R. Finones, *J. Electrochem. Soc.*, **151**, A1279 (2004).
19. S. W. Oh, H.J. Bang, S.-T. Myung, Y.C. Bae, S.M. Lee, Y.-K. Sun, *J. Electrochem. Soc.*, **155**, A414 (2008).
20. J. R. Ying, C. Y. Jiang and C. R. Wan, *J. Power Sources*, **129**, 264 (2004).
21. P. P. Prosini, M. Carewska, S. Scaccia, P. Winsniewski, S. Passerini and M. Pasquali, *J. Electrochem. Soc.*, **149**, 886 (2002).
22. S. T. Myung, S. Komaba, N. Hirosaki, H. Yashiro and N. Kumagai, *Electrochim. Acta*, **49**, 4213 (2004).
23. C. Y. Lee, H. M. Tsai, H. J. Chuang, S. Y. Li, P. Lin and T. Y. Tseng, *J. Electrochem. Soc.*, **152**, A716 (2005).
24. Y.-K. Sun, S.-T. Myung, C.-S. Yoon and D.-W. Kim, *Electrochem. Solid-State Lett.*, **12**, A163 (2009).
25. C. K. Park, S. B. Park, S. H. Oh, H. Jang and W. I. Cho, *Bull. Korean Chem. Soc.*, **32**, 836 (2011).